Analysis of the Very Long Baseline Experiment Using GLoBES

Christine Lewis

August 12, 2005

1 Introduction

Historically, the existence of neutrinos was proposed as a means of preserving conservation of energy in β-decays [1][2]. Until relatively recently, however, there was little known about the behavior of neutrinos except that fewer of them appeared to be coming from the sun than the Standard Solar Model predicted. Over the past decade, several experiments have collected compelling evidence that explains the solar deficit in terms of neutrino oscillations [3].

Neutrino oscillations can be described by six parameters: three mixing angles, θ_{12}, θ_{23}, and θ_{13}, two mass differences Δm_{21}^2, and Δm_{31}^2, and a CP-violation phase δ_{CP}[4]. Currently, θ_{12} and Δm_{21}^2, referred to as the solar parameters, are fairly well measured [3, 5]. Additionally, the atmospheric parameters θ_{23} and $|\Delta m_{31}^2|$ have been measured, although the sign of Δm_{31}^2 is unknown [6, 7]. There is an upper limit on the value of θ_{13} at about $10°$ [8] and δ_{CP} is completely unknown.

The Very Long Baseline Experiment (VLB) is a proposed experiment which would send a broadband neutrino beam over a distance of a few thousands of kilometers [9]. Such an experiment would be able to measure the atmospheric parameters with greater precision and it would have increased sensitivity to the unknown parameters. In one possible set-up, which I used for the calculations discussed in this paper, the beam would be created at the AGS facility at Brookhaven National Laboratory [10, 11]. The neutrinos would be detected by a 500 kiloton water Cherenkov detector about 2540 kilometers away in the Homestake mine in South Dakota. The beam would run for five years with neutrinos (1 MW proton beam) and five years with anti-neutrinos (2 MW proton beam).

In this paper I will discuss the use of the General Long Baseline Experiment Simulator (GLoBES) [12] software in the analysis of the VLB experiment. Calculations include measurements of the atmospheric parameters, sensitivities to $\sin^2 2\theta_{13}$ and δ_{CP} the excluded region for $\sin^2 2\theta_{13}$ in the case where $\theta_{13} = 0$, and the VLB's sensitivity to the mass hierarchy. Additionally, I will use GLoBES to see how a proposed future reactor experiment measuring of $\bar{\nu}_e$ disappearance would contribute to the VLB measurement of $\sin^2 2\theta_{13}$.

2 GLoBES

An experimental set-up can be described in a file written in the abstract experiment definition language (AEDL) provided by GLoBES. A C-library is then used to generate event spectra based on these definition files. GLoBES can compare the spectra resulting from an arbitrary set of "true" oscillation parameters to the spectra that would be seen for other values of the parameters. In this way, sensitivity to of any of the six parameters can be calculated. In the following sections I will briefly summarize some of the inputs in the VLB definition files.

2.1 Experiment Conditions

I used two different experiment definitions, one that described neutrino running and one that described anti-neutrino running [13]. The key features of the experiment are a 2540km baseline with matter density given by the average over that distance by the PREM [14] profile, five years of running time, and a 500 kT water Cherenkov detector in both cases. GLoBES input files also require a normalization factor in order to ensure that correct units are used for the fluxes. In both VLB files this factor is set to 2.6054e12. Neutrinos are grouped into 60 reconstructed energy bins of 0.125 GeV between 0.5 GeV and 8 GeV and two 2 GeV bins between 8 GeV and 12 GeV. The difference in basic conditions between neutrino running and anti-neutrino running is that the former uses a 1MW proton beam, while the power is increased to 2MW for the latter. In both cases the incident energy of the proton beam is 28 GeV.

2.2 Flux

The neutrino/anti-neutrino fluxes versus energy are given in separate input files. Each file has seven columns, the first gives an energy and the remaining six give the fluxes of ν_e, ν_μ, ν_τ, $\bar{\nu}_e$, $\bar{\nu}_\mu$, and $\bar{\nu}_\tau$ respectively. For the VLB there are two such flux files, one applies to neutrino running and the other to anti-neutrino running. τ flavors are not taken into account in either file. Also, in the file describing neutrino running, *all* anti-neutrino fluxes are neglected. $\bar{\nu}_\mu$ contamination is a few percent of the ν_μ flux; the total background for neutrino running may be slightly lower than it would actually be. However, this fraction is much smaller than the presumed error on the background (see Section 2.6). The flux as a function of energy for both neutrino types can be seen in Figure 1.

2.3 Energy Resolution

The energy smearing matrices used to get the reconstructed energy for different kinds of events have dimensions 62x62 and range, in both dimensions, from 0.5 GeV to 12 GeV. Abbreviated versions of these matrices, which contain only the non-zero entries, are stored in separate text files. The columns in these files correspond to true energies and add (approximately) to one. The 0.5 - 8 GeV parts of energy resolution matrices for four types of events are plotted in Figure 2.
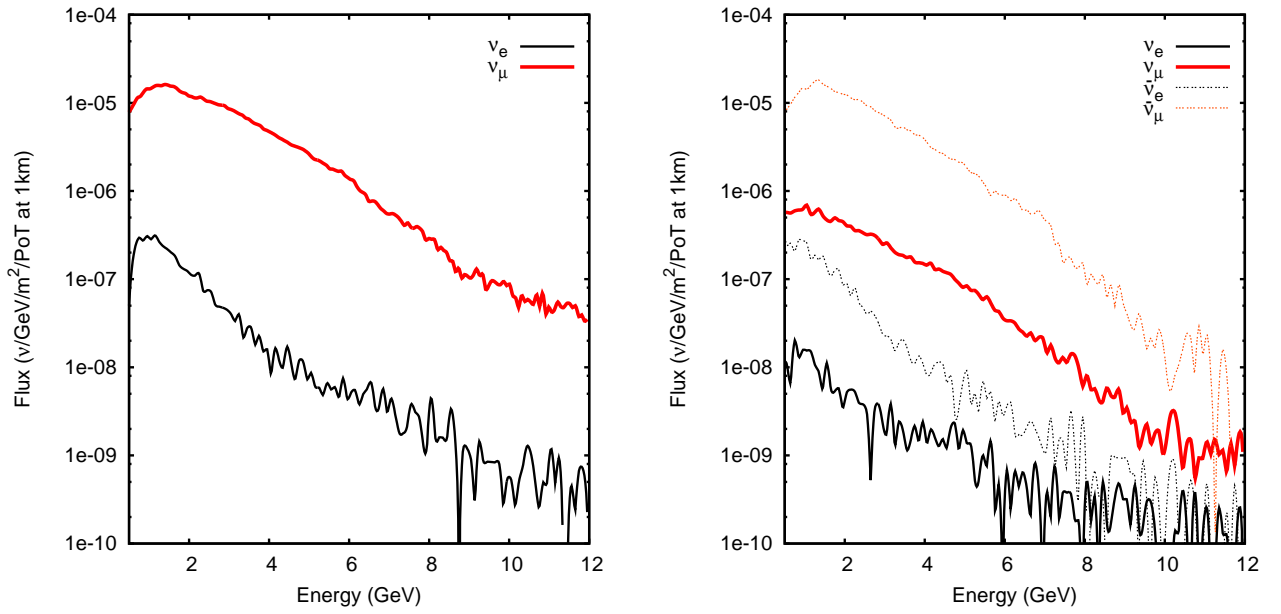
Figure 1: The flux file for neutrino running as defined in BNL.dat (left) and anti-neutrino running as defined in BNLminus.dat (right). Units used are: $\nu/\mathrm{GeV}/\mathrm{m}^2/\mathrm{proton}$ on target at 1 km. Note that there is no anti-neutrino flux in the file describing neutrino running. The discontinuous behavior is a result of statistical uncertainty in the predictions.
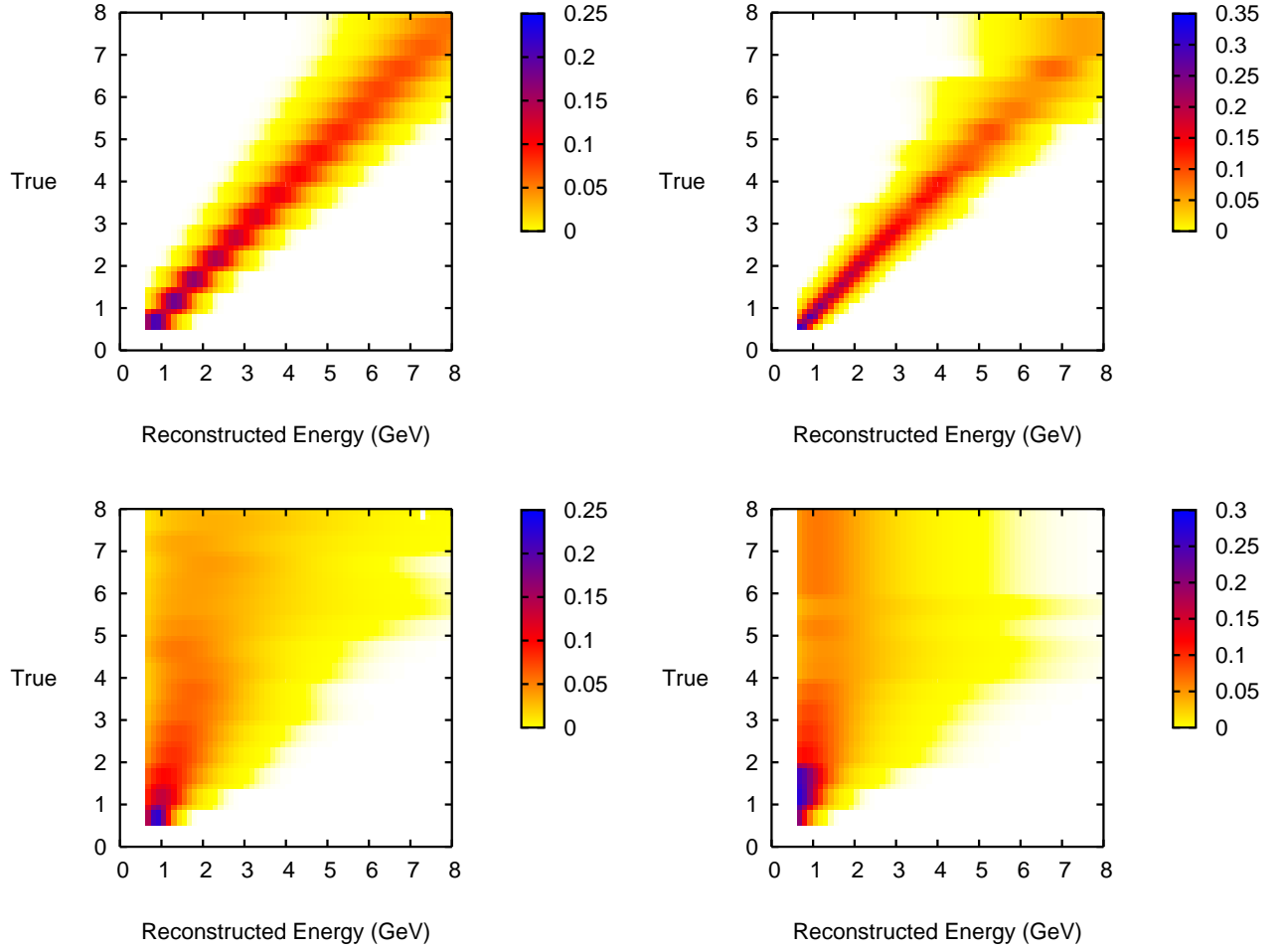
Figure 2: Plots of energy resolution for (clockwise from top left) disappearance, beam, pion, and neutral current events as defined in Table 2. The color indicates the probability that an event will be reconstructed at a certain energy (along the horizontal axis) given its true energy (along the vertical axis).

2.4 Cross sections

Event cross sections are given in files similar to the fluxes, except the first column is the log (base 10) of the energy and there are 1001 lines. The energy range is approximately 0.1-100 GeV divided into 1000 even steps of $\log_{10} E$. The files for charged current and quasi-elastic cross sections were provided with GLoBES [15, 16]. Plots of all cross section files are in Figure 3.
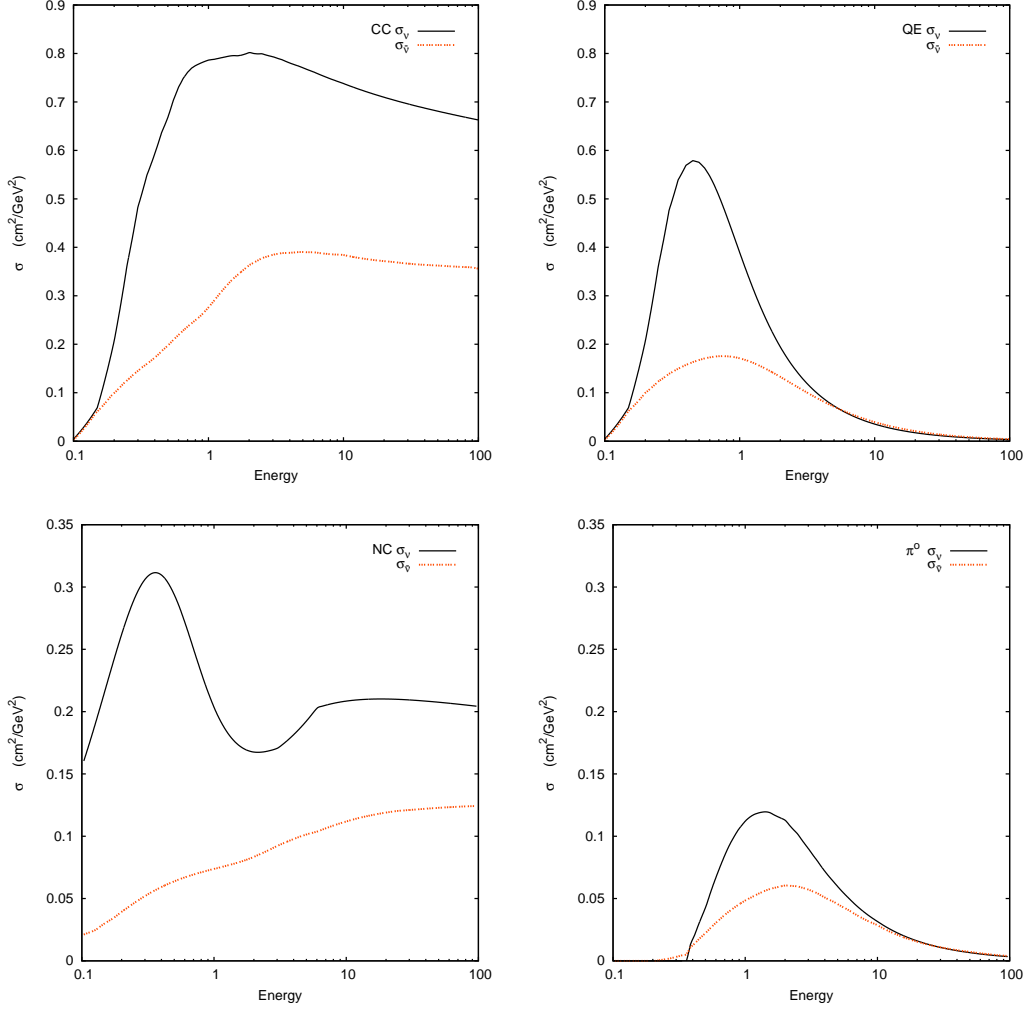

Figure 3: Cross section plots for (clockwise from top left) charged current [15], quasi-elastic [16], π^0, and neutral current interactions. At the energies shown there is no significant difference between ν_e and ν_μ or $\bar{\nu}_e$ and $\bar{\nu}_\mu$, and τ flavor neutrinos are not included in the fluxes. Therefore the black (solid) line gives the cross section for neutrinos and the red (dashed) line for anti-neutrinos.

2.5 Channels

The experiment definition files contain information on various physical processes, called channels. The channels incorporate information from flux files, cross section files and energy smearing matrices as shown in Table 1. Additionally, each channel definition specifies the CP sign, initial flavor, and final flavor of the neutrinos involved. For the neutral current and pion backgrounds, oscillations are not taken into account for ν_μ's because neutral current interactions do not depend on neutrino flavor.

Channel name	Initial→Final flavor	Cross section[†]	Energy smearing[‡]
nc_bg	$\nu_\mu \to \nu_\mu$ (no osc.)	NC	nc
pi_bg	$\nu_\mu \to \nu_\mu$ (no osc.)	PI	pi0
nu_e_beam	$\nu_e \to \nu_e$	CC	beam
nu_e_signal	$\nu_\mu \to \nu_e$	QE	signal
nu_mu_signal	$\nu_\mu \to \nu_\mu$	QE	dis
nu_mu_bg	$\nu_\mu \to \nu_\mu$	QE	mpip
anc_bg	$\bar{\nu}_\mu \to \bar{\nu}_\mu$ (no osc.)	NC	anc
api_bg	$\bar{\nu}_\mu \to \bar{\nu}_\mu$ (no osc.)	PI	api0
anu_e_beam	$\bar{\nu}_e \to \bar{\nu}_e$	CC	abeam
anu_e_signal	$\bar{\nu}_\mu \to \bar{\nu}_e$	QE	asinal
canc_bg	$\nu_\mu \to \nu_\mu$ (no osc.)	NC	ancc
capi_bg	$\nu_\mu \to \nu_\mu$ (no osc.)	PI	api0c
canu_e_beam	$\nu_e \to \nu_e$	CC	abeamc
canu_e_signal	$\nu_\mu \to \nu_e$	CC	asignalc
anu_mu_signal	$\bar{\nu}_\mu \to \bar{\nu}_\mu$	QE	adis
anu_mu_bg	$\bar{\nu}_\mu \to \bar{\nu}_\mu$	QE	ampip
canu_mu_signal	$\nu_\mu \to \nu_\mu$	CC	adisc
canu_mu_bg	$\nu_\mu \to \nu_\mu$	CC	ampipc

Table 1: The top section is for neutrino running and uses BNL.dat as its flux file. The bottom section is for anti-neutrino running and uses BNLminus.dat [13]. Cross section files are the same for both neutrino and anti-neutrino running.
[†] See Figure 3 for plots of the cross sections.
[‡] See Figure 2 for plots of the first four energy resolution files.

2.6 Rules

Rules contain signal and background components as well as information about the systematic errors for the events falling under each rule. In the VLB there are two rules: ν_e (or $\bar{\nu}_e$) appearance and ν_μ (or $\bar{\nu}_\mu$) disappearance. The signal and background for a rule is calculated based on a fraction (the post-smearing efficiency) of events from one or more channels. Both the neutrino and anti-neutrino definition files use two rules. The rule definitions are given in Table 2.

The systematic errors placed on the signal for all rules in both experiment definitions are a normalization error of 1%. Backgrounds in both definitions have a 10% normalization error. Additionally, there is an error on the shape, or "tilt," of 0.01% on all signal and background errors.

	Neutrino running				
Rule	ν_e-appearance			ν_μ-disappearance	
	fraction	channel		fraction	channel
signal	0.12	nu_e_signal		0.12	nu_mu_signal
background	0.26*0.032	nc_bg		0.14*0.18	nu_mu_bg
	0.033*0.0057	pi_bg			
	0.021	nu_e_beam			
	Anti-neutrino running				
Rule	$\bar{\nu}_e$-appearance			$\bar{\nu}_\mu$-disappearance	
	fraction	channel		fraction	channel
signal	0.88*0.11868	anu_e_signal		0.985*0.91*0.118	anu_mu_signal
background	0.01138*0.0462	anc_bg		0.61*0.3*0.084	anu_mu_bg
	0.0185*0.0081	api_bg		0.9*0.047	canu_mu_signal
	0.88*0.04	anu_e_beam		0.8*0.216*0.06	canu_mu_bg
	0.8*0.262*0.008	canc_bg			
	13.5*0.0185*0.0016	capi_bg			
	0.88*0.036	canu_e_beam			
	0.9*0.047	canu_e_signal			

Table 2: The composition of ν_e appearance and ν_μ disappearance rules for neutrino-running (top) and anti-neutrino running (bottom). The channels are defined in Table 1.

2.7 Oscillation Parameters

The oscillation parameters are not defined in the experiment definition files. Instead, they can be set to arbitrary values when using GLoBES to make calculations. It is also possible to put errors on the precision of previously determined parameters. GLoBES's minimizer uses these errors to add a penalty to the calculated value of χ^2. For most of my calculations the solar and atmospheric parameters and their respective errors are set to the values shown in Table 3. These are the more or less the currently known values of the solar and atmospheric parameters as determined by a recent global fit to neutrino oscillation data [17]. The values used for $\sin^2 2\theta_{13}$ and δ_{CP} vary and are explained with the calculations. Additionally, there is a 5% uncertainty put on the mass density for calculations where errors are relevant.

Parameter	Value	Error
$\sin^2 2\theta_{12}$	0.86	8.3%
$\sin^2 2\theta_{23}$	1	13%
Δm_{21}^2	8e-5	5%
Δm_{31}^2	2.5e-3	10%

Table 3: The values used for the measured oscillation parameters and the errors placed on their values when using the GLoBES minimizer.

3 ν_μ Disappearance

3.1 Spectra

To generate the disappearance spectra, shown in Figure 4, I called GLoBES from a command line. The rates returned take into account the applicable backgrounds and include efficiencies and energy smearing (see Table 2. The solar and atmospheric oscillation parameters are set to the values in Table 3. The values of $\sin^2 2\theta_{13}$ and δ_{CP} are both zero. As this calculation does not involve minimization, input errors were not used.
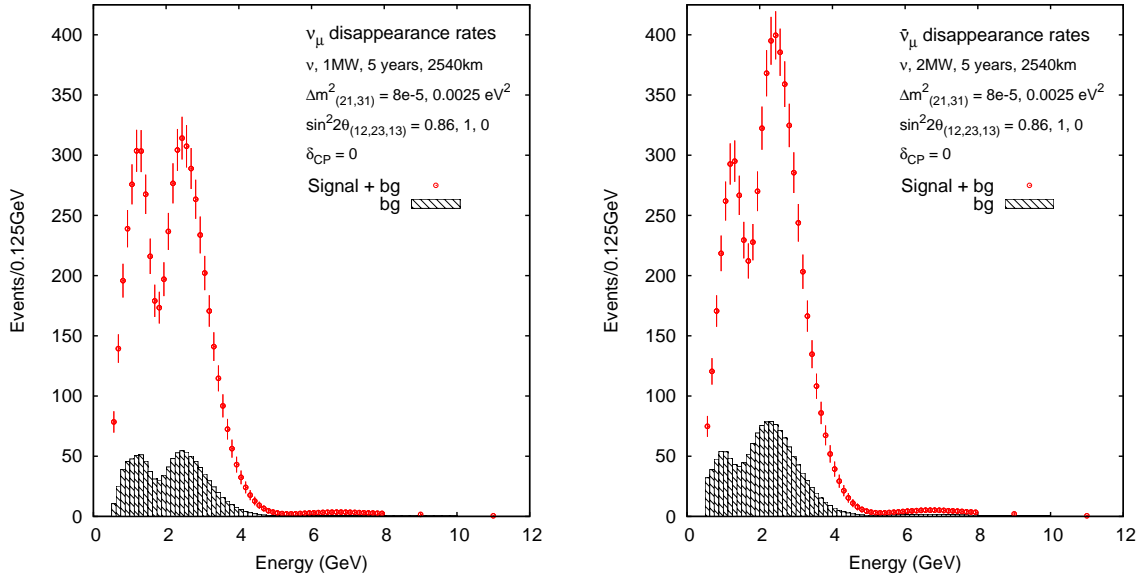

Figure 4: ν_μ (left) and $\bar{\nu}_\mu$ (right) disappearance spectra as functions of the reconstructed neutrino energy. The hatched histogram shows the background contribution. The data points give the total signal and background. The error bars correspond to the expected statistical error for that bin. Values of the oscillation parameters are also shown.

3.2 Measurement of atmospheric parameters

For the measurement of the atmospheric parameters, $\sin^2 2\theta_{23}$ and Δm_{31}^2, the solar parameters and $\sin^2 2\theta_{13}$ and δ_{CP} were set to the same values used when calculating the disappearance spectra. I tested nine combinations of θ_{23} and Δm_{31}^2. GLoBES was permitted to vary the mass density within 5% and all parameters except Δm_{31}^2 and $\sin^2 2\theta_{23}$ within 5-10% errors from the central values to get the minimum χ^2. This was then projected onto the $\sin^2 2\theta_{23}$-Δm_{31}^2 plane. The errors on $\sin^2 2\theta_{13}$ and δ_{CP} were set to zero, which is equivalent to leaving them completely free. However they have no effect on the disappearance spectra, so this does not make a difference in the measurement. The minimization is performed for approximately 2500 combinations of θ_{23} and Δm_{31}^2 around their true values. θ_{23} is used instead of $\sin^2 2\theta_{23}$ to avoid problems that might be caused by attempting to test a value of $\sin^2 2\theta_{23} > 1$. The 1σ and 3σ contours of the resulting surface for 2 d.o.f. are shown in Figure 5. The contours show a 1.5-3.5% measurement of $\sin^2 2\theta_{23}$ and a 2% measurement of Δm_{31}^2 at 3σ (95.45% C.L.) after five years of neutrino running.
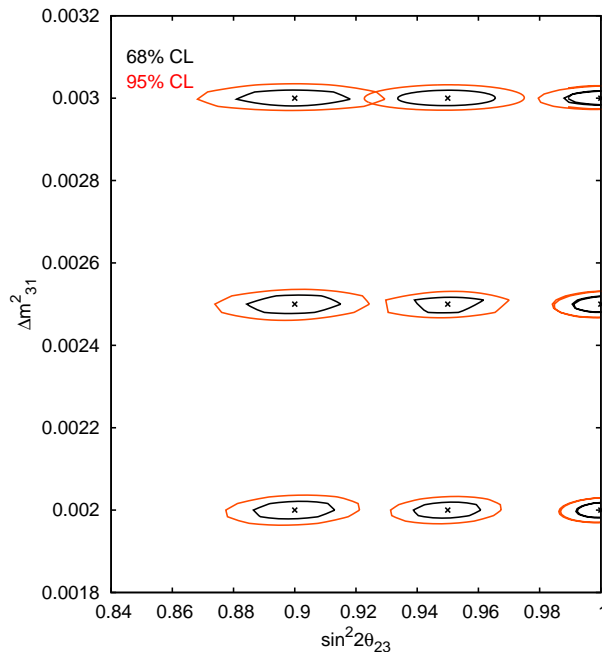

Figure 5: The measurement of $\sin^2 2\theta_{23}$ and Δm_{31}^2 for given true values at 1σ and 3σ after five years of neutrino running. Systematics include a 1% normalization error on the signal and a 10% normalization error on the background.

9

4 ν_e Appearance

4.1 Spectra

The appearance spectra (Figure 6) are generated essentially the same way as the disappearance spectra. In this case $\sin^2 2\theta_{13}$ and δ_{CP} were varied and the other parameters were set to the values in Table 3. However, the reconstructed energy bins were added to get event rates per 0.5 GeV instead of per 0.125 GeV.

The backgrounds are made up of the interactions described in Table 2 under ν_e and $\bar{\nu}_e$ appearance background.
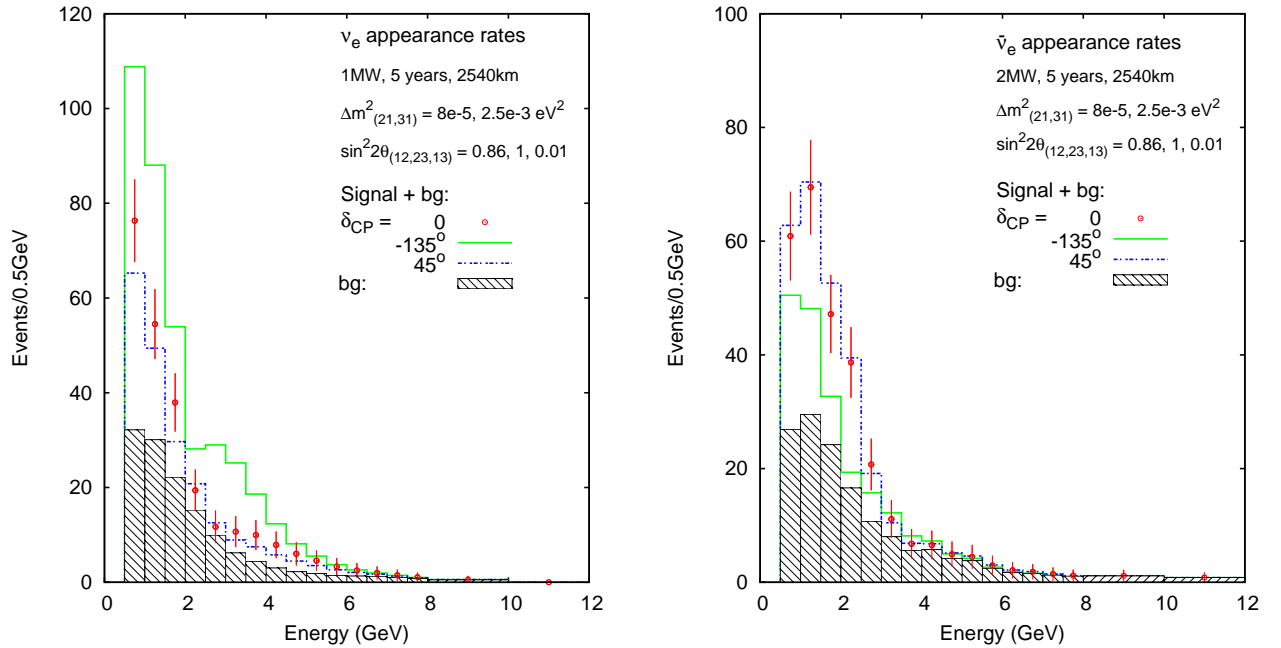

Figure 6: ν_e(left) and $\bar{\nu}_e$(right) appearance spectra for five years each of neutrino and antineutrino running for $\sin^2 2\theta_{13}= 0.01$. The hatched histogram shows the background. The data points show signal and background rates for $\delta_{CP}= 0$. The error bars give the expected statistical error for each bin. The green (solid) and blue (dashed) lines show signal and background rates for $\delta_{CP}= -135°$ and $45°$, respectively. The values of the other parameters are also shown.

4.2 Measurement of $\sin^2 2\theta_{13}$ and δ_{CP}

I tested 21 combinations of $\sin^2 2\theta_{13}$ and δ_{CP} with the solar and atmospheric parameters set to the values described in Table 3. All parameters except $\sin^2 2\theta_{13}$ and δ_{CP} were minimized over with the errors listed in Table 3. Additionally, there was a 5% uncertainty placed on the matter density. For each combination of true values, I tested about 2400 values of

$\log_{10} \sin^2 2\theta_{13}$ and δ_{CP} around the central values. Figure 7 shows that for $\sin^2 2\theta_{13}$ around 0.02 (0.1), a measurement could be made within 50% (20%)at 90% C.L. and δ_{CP} could be measured to 30-50° (20-40°) at 90% C.L after five years of neutrino running.
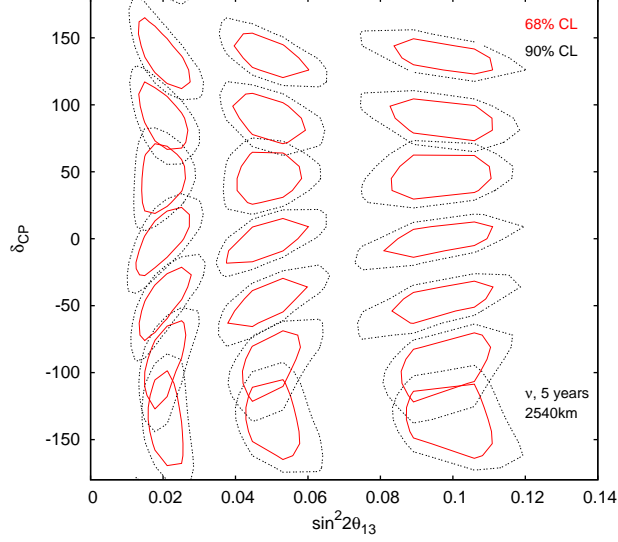

Figure 7: Measurement of $\sin^2 2\theta_{13}$ and δ_{CP} after five years of neutrino running. This plot assumes normal mass ordering and uses the parameter values and errors listed in Table 3. Systematics include a 1% normalization error on the signal and 10% normalization error on the background.

4.3 $\sin^2 2\theta_{13}$ exclusion

The three exclusion plots in Figure 8 show the values of $\sin^2 2\theta_{13}$ that could be ruled out if $\sin^2 2\theta_{13}$ were zero[1] for a given value of δ_{CP}. The plots were made by fixing δ_{CP} and letting $\sin^2 2\theta_{13}$ increase until the value of χ^2 reached the 95% and 99% confidence levels for 2 d.o.f. This was repeated with 60 values of δ_{CP} between $-180°$ and $180°$ for both "normal" ($\Delta m_{31}^2 > 0$) and reversed ($\Delta m_{31}^2 < 0$) orderings of the mass heirarchy. Two degrees of freedom are used because they allow one to determine the excluded region of $\sin^2 2\theta_{13}$ as a function of δ_{CP}. After five years of neutrino running, the VLB would be able to exclude $\sin^2 2\theta_{13}$ above 0.07 if $\Delta m_{31}^2 < 0$. If $\Delta m_{31}^2 > 0$ it would be able to exclude $\sin^2 2\theta_{13}$ above approximately 0.01. After an additional five years of running with anti-neutrinos $\sin^2 2\theta_{13}$ would be excluded above 0.006 regardless of the mass hierarchy.

---

[1]Technically, I did not use 0 for $\sin^2 2\theta_{13}$ but set $\theta_{13} = 0.0001$. So, $\sin^2 2\theta_{13}$ is on the order of 10^{-8}.
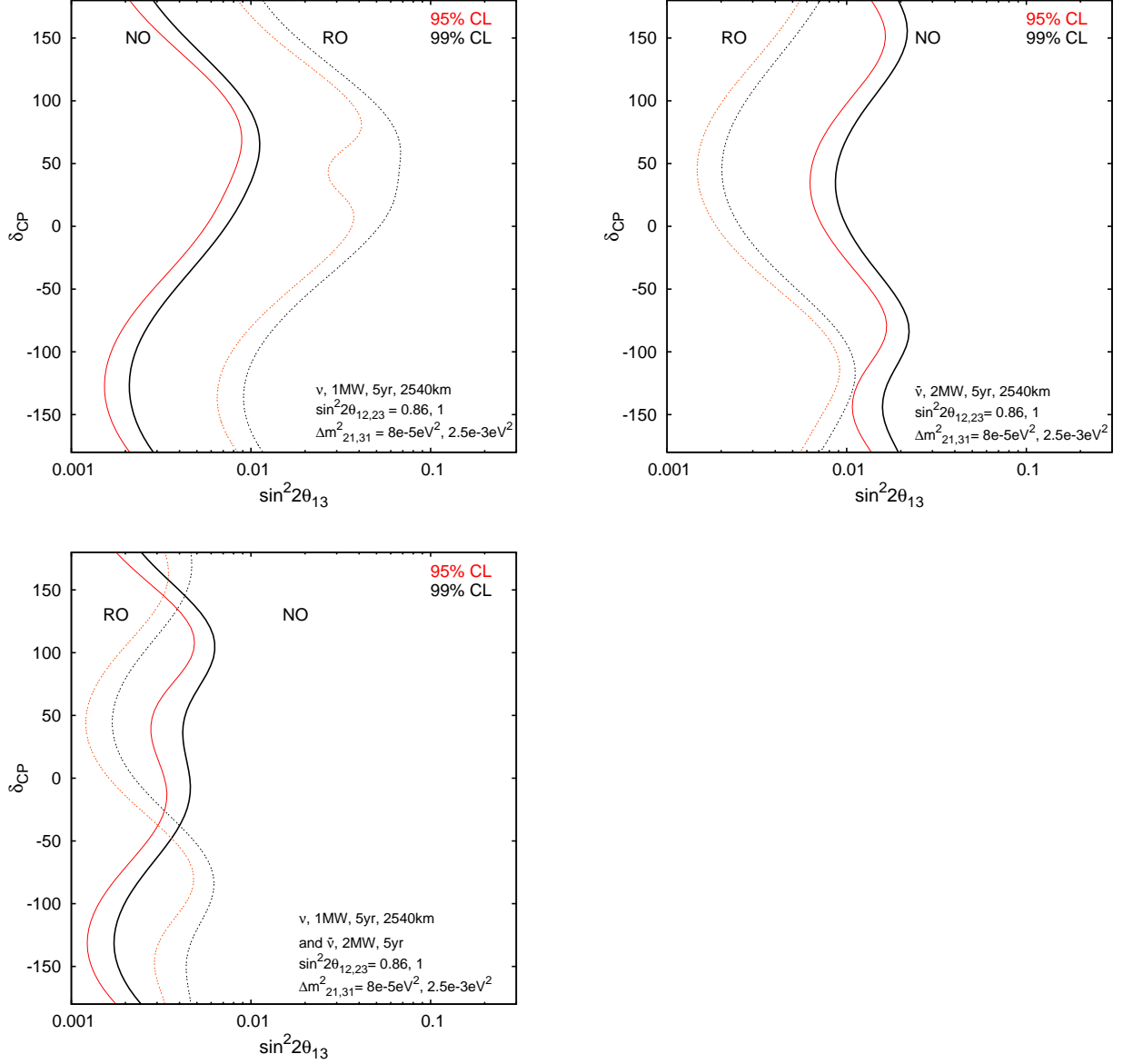
Figure 8: Exclusion plots for neutrino, anti-neutrino, and combined running. The solid lines (NO) correspond to $\Delta m_{31}^2 > 0$ and the dashed lines (RO) correspond to $\Delta m_{31}^2 < 0$. The region to the right of a given line are the values of $\sin^2 2\theta_{13}$ that can be excluded at 95.45% C.L. (red) and 99% C.L. (black) for 2 d.o.f. The parameter values and errors used were those listed in Table 3. Additionally, there is a 5% uncertainty on the matter density. The background channels and rules are described in Tables 1 and 2 respectively and there is a 10% normalization error on the backgrounds (see Section 2.6).

4.4 Sensitivity to the mass hierarchy

To make an estimate of the VLB experiment's sensitivity to the sign on Δm^2_{31}, I got the ν_e appearance rates for five values of $\sin^2 2\theta_{13}$ with $\delta_{CP} = 0$. The values used for the other parameters are the ones in Table 3 except for Δm^2_{21} which was set to 7.3×10^{-5} eV^2. Also, no minimization was done, so the errors on the parameter values are not relevant. Instead of using the total signal and background rates, the calculation is made based on the number of events with reconstructed neutrino energy between 2.44 and 7.94 GeV. At higher energies the background is relatively higher than it is in the central region. At lower energies there is also little sensitivity to the mass hierarchy. To calculate the sensitivity, the following equations were used:

$$\sigma_{\pm} = \sqrt{sig_{\pm} + bg} \tag{1}$$

$$s = \frac{|sig_+ - sig_-|}{\sqrt{\sigma_+^2 + \sigma_-^2}} \tag{2}$$

where sig_+ (sig_-) is the number of expected signal events for positive (negative) Δm^2_{31} and bg is the number of background events. The estimated sensitivity to the mass hierarchy for five years of either neutrino or anti-neutrino running is shown in Figure 9.
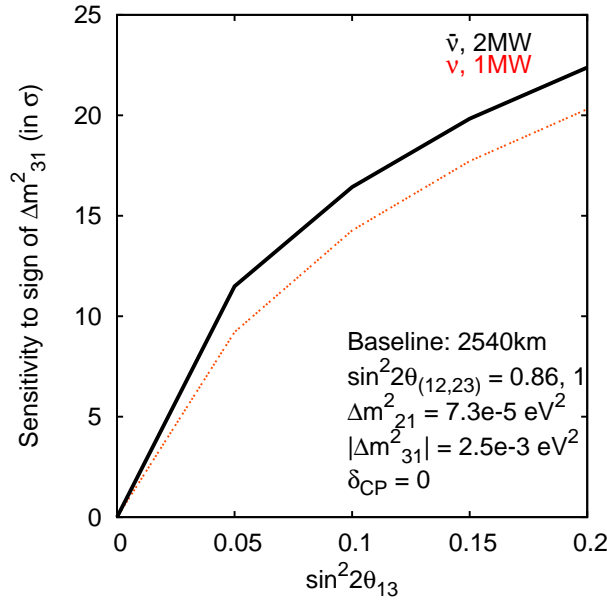

Figure 9: The estimated number of σ to which the mass hierarchy would be determined after 5 years of neutrino running (red, dashed line) or 5 years of anti-neutrino running (black, solid line). The calculation is based on the expected event rates for different mass hierarchies.

5 Combination with reactor experiment

Several reactor experiments are proposed for the near future to attempt to find θ_{13}. For the purpose of comparison, I used GLoBES to calculate the measurement of $\sin^2 2\theta_{13}$ versus δ_{CP} that could be made considering a contribution from both the VLB and a reactor experiment. In this section, I will use $\sin^2 2\theta_{13} = 0.05$ and $\delta_{CP} = 0$.

5.1 Reactor Experiment Conditions

The reactor definition used was Reactor1 [18][21], which is included in the GLoBES 2.0.11 source code. It describes a five year experiment with a 4GW (thermal) source, a target mass of 20 tons, and a baseline of 1.7km. Due to the short baseline, the matter density is neglected by setting its value to 1×10^{-6} gm/cm^3. It has 62 energy bins between 1.8 and 8 MeV. For energy resolution, it uses the inverse beta function provided by GLoBES with $\alpha = 0.05$ and E in GeV:

$$\sigma(E) = \begin{cases} \frac{\alpha\sqrt{E - 8 \times 10^{-4}}}{\sqrt{1000}} & E > 1.8 \times 10^{-3} \\ \alpha \times 10^{-3} & E \leq 1.8 \times 10^{-3} \end{cases} \tag{3}$$

The Reactor1 file describes only one channel; it is for $\bar{\nu}_e \rightarrow \bar{\nu}_e$ and uses its own cross section file [21] in addition to the energy resolution function described above. There is only one rule. Its signal is 100% of events in the above channel with a 0.8% normalization error and a 0.5% calibration error. Its background is 5×10^{-6}% of the above channel with normalization and calibration errors of 1×10^{-4}%.

5.2 The Reactor Measurement of $\sin^2 2\theta_{13}$

Figure 10 shows that the reactor experiment would measure $\sin^2 2\theta_{13} = 0.05 \pm 0.02$ at 68% C.L. in five years if the true value of $\sin^2 2\theta_{13}$ is 0.05. To make the plot, GLoBES was allowed to minimize over all parameters except $\sin^2 2\theta_{13}$. δ_{CP} was left completely free to vary and the remaining parameters were permitted to vary within the errors given in Table 3.

5.3 Combination of Reactor1 and VLB

Figure 11 shows the measurement that would be made combining neutrino running from the VLB with the reactor experiment and the measurement that would be made by neutrino running from the VLB alone. Both plots used the same minimization, which was equivalent to that used for the reactor running alone except that δ_{CP} is free for these minimizations. As expected, the reactor experiment result does not significantly contribute to the VLB experiment after five years of running. However, a reactor experiment result would be important in deciding the strategy used by the VLB in its first few years.
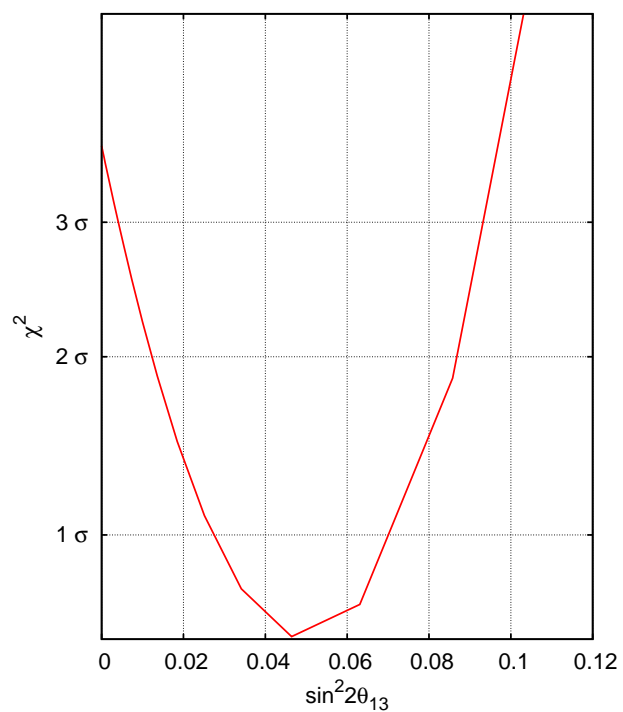
Figure 10: Measurement by the Reactor1 experiment of $\sin^2 2\theta_{13}$ (1 d.o.f.) in the case where $\sin^2 2\theta_{13} = 0.05$ for five years of running. Other parameters are set to the values in Table 3.
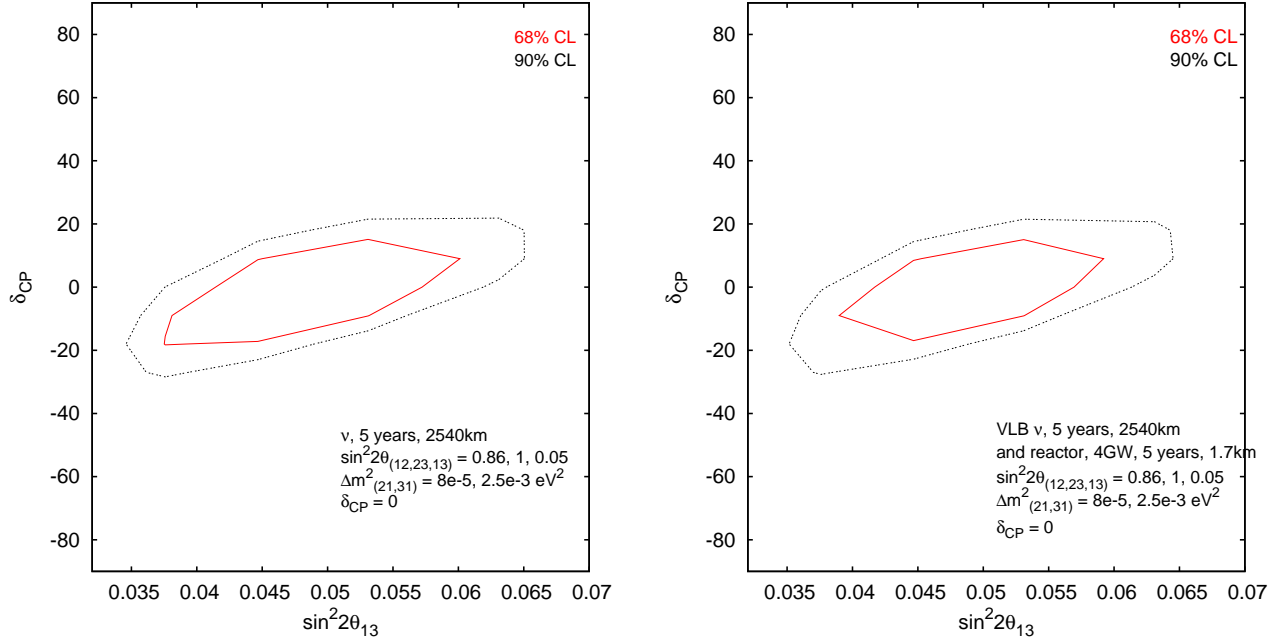
Left plot:

80
60
40
20
0
-20
-40
-60
-80

δ_{CP}

68% CL
90% CL

ν, 5 years, 2540km
$\sin^2 2\theta_{(12,23,13)}$ = 0.86, 1, 0.05
$\Delta m^2_{(21,31)}$ = 8e-5, 2.5e-3 eV^2
δ_{CP} = 0

0.035 0.04 0.045 0.05 0.055 0.06 0.065 0.07
$\sin^2 2\theta_{13}$

Right plot:

80
60
40
20
0
-20
-40
-60
-80

δ_{CP}

68% CL
90% CL

VLB ν, 5 years, 2540km
and reactor, 4GW, 5 years, 1.7km
$\sin^2 2\theta_{(12,23,13)}$ = 0.86, 1, 0.05
$\Delta m^2_{(21,31)}$ = 8e-5, 2.5e-3 eV^2
δ_{CP} = 0

0.035 0.04 0.045 0.05 0.055 0.06 0.065 0.07
$\sin^2 2\theta_{13}$

Figure 11: For the case where $\sin^2 2\theta_{13}$= 0.05 and δ_{CP}= 0 the plot on the left shows the measurement that the VLB would make after five years of neutrino running independent of other experiments. The figure on the right shows what would be measured when combined with the results from the experiment described in Reactor1.glb. In both cases, 2 d.o.f. are used. The parameters are given the values and errors listed in Table 3 and everything is minimized over except for $\sin^2 2\theta_{13}$ and δ_{CP}.

6 Conclusion

In this paper I discussed the use of GLoBES to describe the VLB experiment and to determine its sensitivity to the oscillation parameters for neutrino and anti-neutrino running. I also estimated the sensitivity to the mass hierarchy and the combination of a future reactor experiment's measurement of $\sin^2 2\theta_{13}$ with five years of neutrino running. GLoBES made these calculations fairly straightforward. From the GLoBES calculations it is possible to see that the VLB stands to make an improvement on many measurements of neutrino oscillation parameters.

7 Acknowledgements

References

[1] J. Chadwick, "Distribution in intensity in the magnetic spectrum of the β-rays of radium," Verh. Dtsch. Phys. Ges. **16**, 383 (1914).

[2] W. Pauli, Open Letter to Radioactive Persons, (1930).

[3] Q. R. Ahmad *et al.* [SNO Collaboration], "Direct evidence for neutrino flavor transformation from neutral-current interactions in the Sudbury Neutrino Observatory," Phys. Rev. Lett. **89**, 011301 (2002) [arXiv:nucl-ex/0204008].

[4] M. Freund, "Analytic approximations for three neutrino oscillation parameters and probabilities in matter," Phys. Rev. D **64**, 053003 (2001) [arXiv:hep-ph/0103300].

[5] T. Araki *et al.* [KamLAND Collaboration], "Measurement of neutrino oscillation with KamLAND: Evidence of spectral distortion," Phys. Rev. Lett. **94**, 081801 (2005) [arXiv:hep-ex/0406035].

[6] Y. Ashie *et al.* [Super-Kamiokande Collaboration], "A measurement of atmospheric neutrino oscillation parameters by Super-Kamiokande I," Phys. Rev. D **71**, 112005 (2005) [arXiv:hep-ex/0501064].

[7] E. Aliu *et al.* [K2K Collaboration], "Evidence for muon neutrino oscillation in an accelerator-based experiment," Phys. Rev. Lett. **94**, 081802 (2005) [arXiv:hep-ex/0411038].

[8] M. Apollonio *et al.* [CHOOZ Collaboration], "Limits on neutrino oscillations from the CHOOZ experiment," Phys. Lett. B **466**, 415 (1999) [arXiv:hep-ex/9907037].

[9] M. V. Diwan *et al.*, Phys. Rev. D **68**, 012002 (2003) [arXiv:hep-ph/0303081].

[10] W. T. Weng, M. Diwan, D. Raparia, *et al., BNL-73210-2004-IR*

[11] M. Diwan, "The Case for a Super Neutrino Beam" arXiv:hep-ex/0407047.

[12] P. Huber, M. Lindner and W. Winter, "Simulation of long-baseline neutrino oscillation experiments with GLoBES," Comput. Phys. Commun. **167**, 195 (2005) [arXiv:hep-ph/0407333].

[13] The files 0524BNL.glb and 0524BNLanti.glb were written by Patrick Huber and use flux files created by Milind Diwan. 0524BNLanti.glb was modified to use a 2MW proton beam and the modified file was used.

[14] F. D. Stacey, *Physics of the Earth*, 2nd ed., Wiley, 1977

[15] E. A. Paschos and J. Y. Yu, "Neutrino interactions in oscillation experiments," Phys. Rev. D **65**, 033002 (2002) [arXiv:hep-ph/0107261].

[16] Messier, M., UMI-99-23965

[17] A. Strumia and F. Vissani, "Implications of neutrino data circa 2005," arXiv:hep-ph/0503246.

[18] P. Huber, M. Lindner, T. Schwetz and W. Winter, "Reactor neutrino experiments compared to superbeams," Nucl. Phys. B **665**, 487 (2003) [arXiv:hep-ph/0303232].

[19] H. Murayama and A. Pierce, "Energy spectra of reactor neutrinos at KamLAND," Phys. Rev. D **65**, 013012 (2002) [arXiv:hep-ph/0012075].

[20] K. Eguchi *et al.* [KamLAND Collaboration], "First results from KamLAND: Evidence for reactor anti-neutrino disappearance," Phys. Rev. Lett. **90**, 021802 (2003) [arXiv:hep-ex/0212021].

[21] P. Vogel and J. F. Beacom, "The angular distribution of the neutron inverse beta decay, anti-nu/e + p $\rightarrow$ e+ + n," Phys. Rev. D **60**, 053003 (1999) [arXiv:hep-ph/9903554].